Intracellular membrane association of the N-terminal domain of classical swine fever virus NS4B determines viral genome replication and virulence

Tomokazu Tamura[1], Nicolas Ruggli[2], Naofumi Nagashima[1], Masatoshi Okamatsu[1], Manabu Igarashi[3,4], Junki Mine[1], Martin A. Hofmann[2], Matthias Liniger[2], Artur Summerfield[2], Hiroshi Kida[1,3,4], Yoshihiro Sakoda[1,4*]

[1]Laboratory of Microbiology, Department of Disease Control, Graduate School of Veterinary Medicine, Hokkaido University, Sapporo 060-0818, Japan

[2]The Institute of Virology and Immunology IVI, Sensemattstrasse 293, CH-3147 Mittelhäusern, Switzerland

[3]Research Center for Zoonosis Control, Hokkaido University, Sapporo 001-0020, Japan

[4]Global Station for Zoonosis Control, Global Institution for Collaborative Research and Education (GI-CoRE), Hokkaido University, Sapporo 001-0020, Japan

*Corresponding author

Laboratory of Microbiology, Department of Disease Control, Graduate School of Veterinary Medicine, Hokkaido University, North 18, West 9, Kita-ku, Sapporo 060-0818, Japan

Phone: +81-11-706-5207; Fax: +81-11-706-5273

E-mail: sakoda@vetmed.hokudai.ac.jp

Summary word count: 249

The text word count: 5473, 8 figures

Running title: The N-terminal domain of CSFV NS4B determines virulence

Keywords: CSFV; NS4B; virulence; replication

Contents Category: Animal — Positive-strand RNA Viruses

SUMMARY

Classical swine fever virus (CSFV) causes a highly contagious disease in pigs that can range from a severe hemorrhagic fever to a nearly unapparent disease, depending on the virulence of the virus strain. Little is known on the viral molecular determinants of CSFV virulence. The nonstructural protein NS4B is essential for viral replication. However, the roles of CSFV NS4B for viral genome replication and pathogenesis have not yet been elucidated. NS4B of the GPE$^-$ vaccine strain and of the highly virulent Eystrup strain differ by a total of seven amino acid residues, two of which are located in the predicted trans-membrane domains of NS4B and were described previously to relate to virulence, and five residues clustering in its N-terminal part. In the present study, we examined the potential role of these five amino acids in modulating genome replication and determining pathogenicity in pigs. A chimeric low virulent GPE$^-$-derived virus carrying the complete Eystrup NS4B showed enhanced pathogenicity in pigs. The *in vitro* replication efficiency of the NS4B chimeric GPE$^-$ replicon was significantly higher than that of the replicon carrying only the two Eystrup-specific amino acids in NS4B. *In silico* and *in vitro* data suggest that the N-terminal part of NS4B forms an amphipathic α-helix structure. The N-terminal NS4B with these five amino acid residues associated the intracellular membranes. Taken together, this is the first gain-of-function study showing that the N-terminal domain of NS4B can determine CSFV genome replication in cell culture and viral pathogenicity in pigs.

INTRODUCTION

Classical swine fever is an economically important and highly contagious disease of pigs caused by classical swine fever virus (CSFV) (Lindenbach *et al.*, 2013). The disease can range from a severe hemorrhagic fever to a nearly unapparent disease, depending on the virulence of the virus strain. CSFV belongs to the genus *Pestivirus* of the family *Flaviviridae* together with bovine viral diarrhoea virus (BVDV) and border disease virus. CSFV possesses a single-stranded positive-sense RNA genome of approximately 12.3 kb with one large open reading frame flanked by 5′ and 3′ untranslated regions (UTRs). The genome encodes approximately 4000 amino acids that yield at least 12 cleavage products N^{pro}, C, E^{rns}, E1, E2, p7, NS2, NS3, NS4A, NS4B, NS5A, NS5B through co- and post-translational processing of the polyprotein by cellular and viral proteases (Lamp *et al.*, 2013; Lindenbach *et al.*, 2013). Little is known on the role of the different viral proteins in determining CSFV virulence. Nonstructural proteins NS3–NS5B are essential for pestivirus RNA replication (Behrens *et al.*, 1998). Therefore, these nonstructural proteins at least consist of the viral replication complex together with unknown host factors, the replicating viral RNA and intracellular membranes.

The nonstructural protein NS4B is a 38-kDa intracellular membrane-associated protein of the viral replicase, which is analogous to HCV NS4B and other related members of the family *Flaviviridae* (Hugle *et al.*, 2001; Miller *et al.*, 2006; Weiskircher *et al.*, 2009). However, NS4B is a poorly characterised protein and its roles in CSFV replication and pathogenesis are not well understood. A putative Toll/interleukin-1 receptor-like domain was identified in the C-terminal region of NS4B (Fernandez-Sainz *et al.*, 2010). Mutations in this domain of NS4B in the highly virulent Brescia strain resulted in an attenuated phenotype along with enhanced activation of TLR-7-induced genes. In addition, NS4B harbours an NTPase motif (Gladue *et al.*, 2011), but there is no evidence that modulating the NTPase activity may affect virulence. In BVDV, NS4B can act as a modulator of virus cytopathogenicity (Qu *et al.*, 2001). Our previous study demonstrated that two amino acid residues within the predicted trans-membrane domains of NS4B are involved in viral genome

replication and that they contribute to the pathogenicity of CSFV in pigs (Tamura *et al.*, 2012). These two residues are a part of the seven amino acids that differ in NS4B between the highly virulent Eystrup strain and the GPE$^-$ vaccine strain.

Here, we examined whether the five additional amino acid differences in the N-terminal domain of NS4B would further determine viral genome replication *in vitro* and the pathogenicity of CSFV in pigs. To this end, a chimeric virus and corresponding replicons carrying the complete NS4B of the highly virulent Eystrup strain in a modified GPE$^-$ vaccine strain backbone were generated and analysed for pathogenicity *in vivo* and for replication efficiency in cell culture, respectively. An *in silico* approach was used to predict the localisations of these amino acid residues in the N-terminal domain of NS4B. Intracellular membrane localisation and the association mediated by the N-terminal domain of NS4B were examined.

RESULTS

The N-terminal domain of NS4B of the highly virulent CSFV strain Eystrup confers enhanced pathogenicity to a low virulent GPE$^-$-derived virus.

Our previous studies demonstrated the combination of four amino acid residues in N^{pro} (D_{136}), E2 (A_{830}), and NS4B (A_{2475}/V_{2563}) can confer pathogenicity to the CSFV GPE$^-$ vaccine strain in pigs (Tamura *et al.*, 2014; Tamura *et al.*, 2012) (Fig. 1). These four amino acid residues are conserved in the highly virulent Eystrup strain, although a total of 62 amino acids differ between GPE$^-$ and Eystrup strains. The two amino acid residues in the central part of NS4B (A_{2475}/V_{2563}) are part of a total of seven amino acid differences in NS4B. The remaining five amino acid differences (positions at 2377, 2391, 2398, 2399 and 2414) were observed in the N-terminal domain of NS4B. In order to assess whether the five amino acids differing from the GPE$^-$ strain in the N-terminal domain of Eystrup NS4B contribute to pathogenicity in pigs, NS4B in the low virulent GPE$^-$-derived virus (vGPE$^-$/N136D; T830A; V2475A; A2563V) was replaced with NS4B from the highly virulent Eystrup strain. This chimeric virus was termed vGPE$^-$/N136D; T830A; Eystrup NS4B. Groups of six

10-week-old to 13-week-old pigs were inoculated intranasally with $10^{6.0}$ $TCID_{50}$ of these two GPE$^-$-derived viruses. As a control, six pigs were inoculated with the highly virulent Eystrup strain. Infection with the parental virus (vGPE$^-$/N136D; T830A; V2475A; A2563V) did not result in any clinical symptoms in this trial [Fig. 2(a), left panel]. Nevertheless, the body temperature of these pigs was slightly elevated between days 3 and 7 after infection, and low-level viremia was detected during 2 days [Fig. 2(b) and 2(c), left panels]. In contrast, all six pigs inoculated with the vGPE$^-$/N136D; T830A; Eystrup NS4B virus developed overt clinical manifestations between days 4 and 7 pi, with five out of six pigs showing fever [Fig. 2(a) and 2(b), middle panels]. Viremia was detected during 4 days [Fig. 2(c), middle panel]. Infection with the highly virulent Eystrup strain resulted in severe clinical signs with high and prolonged fever and viremia in all six pigs. Four pigs were euthanized when they reached a clinical score above 18, between days 6 and 7 pi. One pig died unexpectedly on day 8 pi, and one pig recovered by day 14 pi. These data demonstrate that the N-terminal domain of NS4B contributes to pathogenicity of CSFV in pigs. Nevertheless, NS4B of the highly virulent Eystrup virus is not solely responsible for the high pathogenicity of this virus.

The N-terminal domain of NS4B of the highly virulent CSFV strain Eystrup contributes to enhanced RNA replication.

Mono-cistronic and bi-cistronic replicons [Fig. 3(a) and 3(b)] were used to determine the effect on viral RNA replication of the amino acids of NS4B differing between the two strains. In SK-6 cells at 24 h post electroporation, the bi-cistronic replicon carrying NS4B of the highly virulent Eystrup strain (rGPE$^-$-N^{pro}-Luc-IRES-NS3/Eystrup NS4B) resulted in 2-fold higher luciferase activity than the replicon carrying only the two amino acid substitutions in the predicted trans-membrane domains of NS4B (rGPE$^-$-N^{pro}-Luc-IRES-NS3/V2475A; A2563V), and in 5-fold higher luciferase activity than the parental GPE$^-$ virus-derived replicon [Fig. 3(c)]. Consistent with the results obtained with the bi-cistronic replicons, Eystrup NS4B conferred significantly higher *Gaussia* luciferase production to the GPE$^-$-derived mono-cistronic replicon compared with the replicon harbouring only the two

V2475A and A2563V substitutions in GPE$^-$ backbone that was also more efficient at expressing the reporter protein than the replicon representing the parental GPE$^-$ vaccine strain [Fig. 3(b) and 3(d)]. These data indicate that the additional five amino acid differences in the N-terminal domain of Eystrup NS4B contribute to enhanced RNA replication efficiency in cell culture.

The N-terminal domain of NS4B forms a predicted amphipathic α-helix and mediates intracellular membrane association.

Secondary-structure prediction was carried out with the NS4B polyprotein sequence of the GPE$^-$ and Eystrup strains by using several different software. The consensus structures are shown in Fig. 4(a). CSFV NS4B comprises an N-terminal domain (amino acids [aa] of NS4B 1–81), a central part that harbours four predicted trans-membrane segments (TM) (aa 82–245) and a C-terminal domain (aa 246–347). The N-terminal domain contains two predicted α-helices from aa 5 to 30 (α1) and from aa 40 to 81 (α2), respectively. Interestingly, five out of the seven amino acid differences between NS4B of the GPE$^-$ vaccine strain and of the Eystrup strain are located within the 2nd α-helix, α2. This α-helix (aa 40–81) is predicted to have an amphipathic structure [Fig. 4(b)]. In order to elaborate on this, the plasmids were constructed for cytomegalovirus promoter-driven expression of the N-terminal α1-helix (aa 1–39), of the helix α2 (aa 40–81), of the two α-helices together (aa 1–81) and of the full-length NS4B protein, all tagged with the green fluorescent protein (GFP) at the C terminus [Fig. 5(a)]. Then, the hydrophobic face of the helix was genetically disrupted by substitution of charged amino acids from the nonpolar amino acids [Fig. 5(b)]. When these different GPE$^-$-derived GFP-tagged NS4B variants were expressed in SK-6 cells, the fluorescence signal of NS4B(40-81)-GFP, NS4B(1-81)-GFP and NS4B-GFP was located essentially in the cytoplasm, with a tendency towards “dot-like” granular structures, which was clearly different from the pattern observed with NS4B(1-39)-GFP and with GFP alone, showing diffuse distribution in the cytoplasm and nucleus at the late stage of transfection. The fluorescence of helix mutants (HMT) of NS4B(40-81)-GFP and NS4B(1-81)-GFP was diffuse distribution and did not observe the “dot-like”

granular structures at all [Fig. 5(c)]. These results indicate that the putative amphipathic α2-helix (aa 40–81) is an essential segment for alternation of the fluorescent pattern.

A membrane flotation assay was used to further characterise the predicted membrane association of the α2-helix of NS4B. A representative Western blot from a membrane flotation experiment with extracts from SK-6 cells expressing NS4B(40-81)-GFP from the GPE$^-$ strain is shown in Fig. 5(d). Low-density membrane fractions are raised towards the top of the gradient, whereas soluble proteins remain with the denser fractions at the bottom. Accordingly, GFP was retained at the bottom of the gradient (fractions 7 and 8) similar to the cytoplasmic soluble protein glyceraldehyde 3-phosphate dehydrogenase (GAPDH). The GFP-tagged α2-helix of NS4B came up in the low-density fractions 3 and 4 (from the top) of the flotation gradient. This was consistent with the accumulation of the membrane-associated calnexin in the gradient fractions 2 and 3 [Fig. 5(d), bottom panel]. In contrast, the disrupted amphipathic helix mutant of the GFP-tagged α2-helix of GPE$^-$ NS4B [GPE$^-$ NS4B(40-81HMT)-GFP] detected at the soluble fraction. Next, to analyse the membrane association of this segment in more details, membrane flotation was examined after treatments that discriminate between peripheral and integral membrane association. To this end, the postnuclear supernatants from cells expressing NS4B(40-81)-GFP were centrifuged at 100000 × *g*, and the pelleted membranes were subjected to different extraction methods. The GFP-tagged NS4B(40-81) remained in the membrane fraction under physiological conditions and after high-salt and alkaline extractions, while detergent extraction resulted in accumulation of NS4B(40-81)-GFP in the higher density soluble fractions. Taken together, the flotation assays confirmed strong intracellular membrane association of the N-terminal amphipathic α2-helix of NS4B (aa 40–81).

Intracellular membrane association mediated by the N-terminal domain of NS4B is a determinant of CSFV RNA replication in cell culture.

In order to clarify the roles of intracellular membrane association mediated by the N-terminal amphipathic domain of NS4B for RNA replication, the both cistronic replicons carrying the same

mutations for disruption of the amphipathic α-helix were generated. The luciferase activity of the helix mutant (rGPE$^-$-N^{pro}-Luc-IRES-NS3/NS4B HMT) was significantly low compared with the luciferase activity of the parental GPE$^-$ replicon [Fig. 6(a)]. This was similar to that of the replication-deficient replicon, indicating that the replication capability was completely abolished by the mutations. In the mono-cistronic replicon assay, the helix mutant behaved similarly as the replication-deficient replicon [Fig. 6(b)]. Altogether, these data indicate that intracellular membrane association mediated by the N-terminal domain of NS4B is critical for RNA replication in cell culture.

The N-terminal domain of NS4B modulates subcellular localisation.

In order to determine the subcellular distribution of the N-terminal domain of NS4B, co-localisation experiments were performed in SK-6 cells expressing the GFP-tagged fusion proteins. As shown in Fig. 7(a), the fluorescence pattern of the GFP-tagged N-terminal domain of NS4B, NS4B(40-81)-GFP and NS4B(1-81)-GFP, appeared to partially overlap with the endoplasmic reticulum (ER). The co-localisation efficient was the same level of the entire NS4B [Fig. 7(b)]. These data indicate that the N-terminal amphipathic helix determines the subcellular localisation of NS4B.

DISCUSSION

In CSFV, the nonstructural protein NS4B is essential for viral replication (Behrens *et al.*, 1998). Our previous study demonstrated that the two amino acid residues that differ between the vaccine strain GPE$^-$ and its parental strain ALD in the predicated trans-membrane domains of NS4B can modulate viral genome replication and influence the pathogenicity of the virus in pigs (Tamura *et al.*, 2012). Here, we generated GPE$^-$-derived virus carrying the complete NS4B of the Eystrup strain, in order to determine whether the additional five amino acid differences in the N-terminal domain of NS4B may contribute to the different pathogenicity in pigs. The GPE$^-$-derived virus carrying NS4B of the highly virulent Eystrup strain resulted in more severe clinical symptoms, earlier and prolonged

viremia compared with the virus carrying only the two amino acid substitutions in the predicted trans-membrane domains. These data indicated that the N-terminal domain of NS4B may represent a virulence determinant *in vivo*. However, as expected, NS4B from the Eystrup strain did not confer a full high virulent phenotype to the GPE$^-$-derived virus, demonstrating that additional viral proteins and amino acid residues are involved in determining the virulence of the Eystrup strain. In addition, the specific residues identified in this study as critical for determining virulence in pigs are not general virulence determinants in CSFV (Fig. 8). This suggests that the virulence of CSFV is more likely a multi-genic trait determined by a complex interplay of several viral proteins or genes acting in concert as already postulated in previous studies (Leifer *et al.*, 2013; Tamura *et al.*, 2012). To the best of our knowledge, this is the first study to show that the N-terminal domain of CSFV NS4B can confer enhanced pathogenicity to a low virulent virus, which was related to an enhanced viral replication.

The five amino acid residues differing between the GPE$^-$ and Eystrup strains in the N-terminal domain of NS4B clearly determine the RNA replication efficiency of replicons *in vitro*. In previous studies, two types of replicons were utilized for studying RNA replication: Mono-cistronic (Risager *et al.*, 2013) and bi-cistronic (Behrens *et al.*, 1998). The minimal viral elements required for RNA replication by pestiviruses including CSFV are NS3–NS5B, together with the 5′ and 3′ UTRs (Behrens *et al.*, 1998). In addition to these minimal elements, the bi-cistronic replicon carries an artificial internal ribosomal entry site (IRES) derived from the encephalomyocarditis virus (EMCV), a luciferase reporter gene, and the viral auto-protease N^{pro} for optimal translation and processing of the reporter protein. The replicative properties of this replicon may however be modified by the EMCV IRES. For these reasons, a mono-cistronic replicon was included. Comparable results of NS4B-dependent differences in RNA replication were obtained with the two types of replicons, strengthening the data.

The granular fluorescent signal derived from the N-terminal domain of NS4B was partially co-localised with the ER by confocal fluorescence microscopy. In the membrane flotation assay, the

N-terminal domain of NS4B was also bound to the ER in part, suggesting that the ER could be a candidate site of the replication complex in infected cells. However, the major part of the N-terminal domain of NS4B detected the different fractions of the ER marker, calnexin. Thus, further studies will be needed to identify the exact subcellular localisation of the replication complex including the natural NS4B in CSFV infected cells. It was described that BVDV NS4B alone can rearrange the host membrane (Weiskircher *et al.*, 2009) as well as HCV NS4B (Egger *et al.*, 2002), suggesting that pestivirus NS4B might act as a trigger for building replication complex. So far, however, pestivirus replication is considered not to remodel cytoplasmic host cell membranes (Schmeiser *et al.*, 2014) as opposed to HCV which induces organelle-like structures designated as the membranous web where the formation of the viral replication complex is triggered (Romero-Brey *et al.*, 2012) and to other positive-strand RNA viruses (Knoops *et al.*, 2008; Kopek *et al.*, 2007; Spuul *et al.*, 2007; Welsch *et al.*, 2009). Therefore, we hypothesize that the role of pestivirus NS4B may be partially different from that in other members of the *Flaviviridae*. Further studies on the functions of the pestivirus NS4B will allow to clarify how the NS4B-dependent modulation of RNA replication may relate to differences in viral replication, morphogenesis and virulence.

Intracellular membrane association mediated by the N-terminal amphipathic domain of NS4B is essential for RNA replication. This amphipathic structure is conserved among CSFV strains (Fig. 8). Interestingly, the amino acid differences in the N-terminal part of NS4B between the prototype vaccine virus and the highly virulent strain studied here are located on the predicated hydrophilic face of the amphipathic α2-helix. These residues are not conserved with respect to virulence of CSFV, however, the amino acid differences among CSFV strains were found mostly on the hydrophilic face of the amphipathic α2-helix, suggesting that the functional differences observed may depend on subtle structure-related differences in association with host proteins and/or other viral nonstructural proteins, modulating replication complex formation, RNA replication and eventually pathogenicity of the virus in pigs. For HCV, the N-terminal amphipathic α2-helix of NS4B is critical for its polymerization, and thus for its accumulation in organelles (Gouttenoire *et al.*, 2010; Yu *et al.*,

2006). A recent study of HCV demonstrated that hydrophilic amino acids in the N-terminal cytoplasmic NS4B are responsible for virus production (Gouttenoire *et al.*, 2014).

In summary, this is the first study showing the roles of intracellular membrane association mediated by the N-terminal domain of CSFV NS4B in viral RNA replication and pathogenicity in pigs. Further studies are required in order to understand the functionality of the pestivirus replication complex at the molecular level, and how this affects pathogenicity in pigs. Understanding the molecular mechanisms involved in viral replication and pathogenesis will permit designing effective tools for controlling the disease.

METHODS

Ethical statement

The animal experiments described here were approved by the Animal Welfare Committee of the Canton of Berne with the license number BE94/12, and conducted in compliance with the Swiss animal protection law and with the national and international animal experimentation guidelines.

Viruses and cells

The CSFV strains, (vGPE$^-$/N136D; T830A; V2475A; A2563V), (vGPE$^-$/N136D; T830A; Eystrup NS4B) and (vEy-37) which is identical to Eystrup were derived from the full-length cDNA clones, *i.e.*, pGPE$^-$/N136D; T830A; V2475A; A2563V (Tamura *et al.*, 2014), pGPE$^-$/N136D; T830A; Eystrup NS4B and pEy-37 (Mayer *et al.*, 2003), respectively. All of the cDNA-derived viruses were rescued as aforementioned (Moser *et al.*, 1999). The complete genomes of the rescued viruses were verified by nucleotide sequencing to exclude any accidental mutations. SK-6 cells were propagated at 37°C in the presence of 5% CO_2 in Eagle's minimum essential medium (Nissui Pharmaceutical) supplemented with 0.3 mg/ml L-glutamine and 7% horse serum (Life Technologies).

Plasmid constructs

The cDNA clone of the mono-cistronic replicon carrying the *Gaussia* luciferase reporter gene, pGPE$^-$2GL, was constructed from rPad2GL (Risager *et al.*, 2013) by replacing the genome of the Paderborn strain with that of the GPE$^-$ strain applying the In-Fusion® HD Cloning (Clontech) techniques as described previously (Tamura *et al.*, 2012). The cDNA clone of rPad2GL was a gift of T. B. Rasmussen (DTU National Veterinary Institute, Denmark). The infectious cDNA clone (pGPE$^-$/N136D; T830A; Eystrup NS4B) and the replicon cDNA clones (pGPE$^-$-N^{pro}-Luc-IRES-NS3/Eystrup NS4B and pGPE$^-$2GL/Eystrup NS4B) were constructed by replacing NS4B in the backbone with the corresponding gene of the highly virulent strain Eystrup as described above. The cDNA clones of the replication-deficient replicons (pGPE$^-$-N^{pro}-Luc-IRES-NS3/GAA and pGPE$^-$2GL/GAA) encoding the amino acid sequence “GAA” instead of “GDD” in the polymerase active site of the nonstructural protein NS5B (Zhong *et al.*, 1998) were constructed from the replicon cDNA clones, pGPE$^-$-N^{pro}-Luc-IRES-NS3 and pGPE$^-$2GL using the QuikChange XL Site-Directed Mutagenesis Kit (Agilent Technologies) and oligonucleotide primers containing the respective mutations based on the aforementioned standard techniques (Tamura *et al.*, 2012). The cDNA clones of the disrupted amphipathic character in the N-terminal domain of GPE$^-$ NS4B (pGPE$^-$-N^{pro}-Luc-IRES-NS3/NS4B HMT and pGPE$^-$2GL/NS4B HMT) were accordingly generated from the parental clones (pGPE$^-$-N^{pro}-Luc-IRES-NS3 and pGPE$^-$2GL) by mutagenesis described above.

In order to construct the GFP, the NS4B construct with a C-terminal GFP-tag and the truncated versions thereof, the cDNA fragments of the respective regions of the GPE$^-$ and Eystrup strains were obtained using reverse transcription and PCR, and the GFP fragments were cloned into the pCI Mammalian Expression Vector (Promega) with In-Fusion® HD Cloning and appropriate restriction enzymes. Details of the constructs are available on request.

Sequencing

The cDNA clones, *in vitro*-rescued viruses, and expression vectors were completely sequenced

as aforementioned (Tamura *et al.*, 2012). In brief, nucleotide sequencing of the cDNA clones, expression vectors and PCR fragments from viral RNA was performed using a BigDye Terminator v3.1 Cycle Sequencing Kit (Life Technologies) and a 3500 Genetic Analyser (Life Technologies). The sequencing data were analysed using Genetyx®-Network version 12 (Genetyx).

Antibodies and markers

The E2-specific monoclonal antibody (mAb) HC/TC26 (Greiser-Wilke *et al.*, 1990) was kindly provided by I. Greiser-Wilke (Hannover Veterinary School, Hannover, Germany). The mAb against viral NS3, 46/1 was generated previously (Kameyama *et al.*, 2006a). The antibodies against cellular organelles, GAPDH and calnexin were purchased from Cell Signaling Technology and Enzo Life Sciences, respectively. The mAb against GFP was obtained from Santa Cruz Biotechnology. A secondary antibody, FITC-conjugated goat anti-mouse IgG, was purchased from MP Biomedicals, and Alexa Fluor 488 $F(ab')_2$ Fragment of Goat Anti-Mouse IgG (H+L) was obtained from Life Technologies. Fluorescent probes for detecting the ER (ER-Tracker) was purchased from Life Technologies. For counterstaining of the cell nuclei, 4′, 6-diamino-2-phenylindole dihydrochloride (DAPI) was obtained from Dojindo Molecular Technologies.

Virus titration

The virus titres were determined by end-point dilution with SK-6 cells and immunoperoxidase staining using anti-E2 mAb HC/TC 26 or anti-NS3 mAb 46/1 as described earlier (Mittelholzer *et al.*, 1997; Sakoda *et al.*, 1998). The titres were calculated using the Reed and Muench formula and expressed as the 50% tissue culture infective dose ($TCID_{50}$) per ml (Reed & Muench, 1938).

Experimental infection of pigs

In order to assess the pathogenicity of the cDNA-derived viruses, groups of six 10-week-old to 13-week-old Large White specific-pathogen-free (SPF) pigs obtained from the breeding unit of The

Institute of Virology and Immunology (IVI, Switzerland) were inoculated intranasally with $10^{6.0}$ $TCID_{50}$ of the respective viruses. All pigs were kept in separate isolation units in the BSL-4 facility of the IVI. The body temperature and clinical scores were monitored daily according to a defined scoring system as described previously (Mittelholzer *et al.*, 2000). Whole blood was collected for serum preparation at 3 days before infection and on days 3, 4, 5, 6, 7, 10 and 12 post-inoculation (pi). The pigs that survived the infection were euthanized on day 14 pi. The virus titres in the serum samples were expressed as the $TCID_{50}$ ml^{-1}.

Luciferase assay

Luciferase assays using bi-cistronic replicons were conducted as previously described (Tamura *et al.*, 2012). In brief, $10^{6.0}$ SK-6 cells were electroporated with 1 µg of replicon RNA. Electroporation was performed at 200 V and 500 µF. At different times after transfection, cell extracts were prepared with 200 µl of passive lysis buffer, and the firefly luciferase activity was measured using a Luciferase Assay System (Promega) and a Lumat LB9507 luminometer (Berthold).

Luciferase assays with mono-cistronic replicons were performed as aforementioned, with some modifications (Risager *et al.*, 2013). Electroporation was conducted under the conditions described above. At the time indicated, 50 µl of cell medium was harvested from the supernatants of cells transfected with replicons, which was then frozen at −20°C. After thawing, 20 µl of the cell medium was analysed to determine the *Gaussia* luciferase activity using *Renilla* luciferase substrate and a Lumat LB9507 luminometer.

The results representing the luciferase activities that were compared with the luciferase activity of the replicon devoid of polymerase activity at the initial timepoints were measured on the basis of three independent experiments.

Immunofluorescence assay

SK-6 cells were transfected with the expression vectors using Lipofectamine 3000 (Life Technologies) and Opti-MEM (Life Technologies), according to the manufacturer's protocol. At the time indicated, SK-6 cells grown on an eight-well chamber slide (Matsunami) were fixed and stained as aforementioned (Sharma *et al.*, 2012; Yamasaki *et al.*, 2012). Anti-GFP mAb as the primary antibody was used at a concentration of 1 mg ml^{-1}. As the secondary antibodies, FITC-conjugated goat anti-mouse IgG (1: 2500) or Alexa-Fluor-conjugated IgG (1: 1000) were used. In order to counterstain the cell nuclei, the cells were incubated for 30 min with 2 μg DAPI ml^{-1} in PBS at room temperature. For labeling the cell organelle, the cells were grown on 35-mm glass-based dishes (IWAKI) and washed with PBS, before staining for 30 min with 100 mM ER-Tracker in complete medium at 37°C with 5% CO_2. The cells were then washed twice with PBS and pre-warmed PBS was added. The fluorescent cells were analysed with a BZ-9000 (KEYENCE) microscope and a BZ-II Analyzer (KEYENCE). The confocal fluorescent images were acquired using Zeiss LSM700 (Carl Zeiss) microscopes (upright and inverted) and ZEN 2012 (Carl Zeiss). Quantitative co-localisation analysis was performed as described elsewhere (Dunn *et al.*, 2011). The co-localisation ratio of the GFP signals with the organelle marker that represents a co-localisation coefficient was quantified using ZEN 2012 software.

Membrane flotation assay

SK-6 cells were grown on 10-cm dishes overnight and transfected with the GFP-tagged NS4B and truncated vectors or with the control GFP constructs according to the conditions described above. At 30 h post-transfection (pt), the cells were re-suspended in hypotonic buffer (10 mM Tris-HCl [pH 7.5], 10 mM KCl, 5 mM $MgCl_2$) containing a protease inhibitor (Complete Mini, Roche). The cells were then disrupted by 20 passages through a 25G needle with 1ml syringe, ensuring approximately 90% disruption. The samples were spun at 1000 × *g* for 5 min at 4°C to pellet the cellular debris and nuclei, thereby obtaining postnuclear supernatants. A discontinuous iodixanol (OptiPrep, Alere Technologies AS) gradient (5%, 25% and 30%) was layered on top of the samples,

followed by centrifugation at 230140 × *g* for 24 h at 4°C in a P40ST Rotor (Hitachi Koki). In total, eight equal fractions were collected from the top to bottom. Each fraction was precipitated with methanol-chloroform and analysed by sodium dodecyl sulfate-polyacrylamide gel electrophoresis followed by immunoblotting using anti-GFP, anti-GAPDH and anti-calnexin as described previously (Kameyama *et al.*, 2006b). For the membrane dissociation experiments, the postnuclear supernatants were adjusted to 0.25 M sucrose and centrifuged at 100000 × *g* for 45 min at 4°C. The pellet containing the membranes and their associated proteins was re-suspended in either high salt buffer (1 M NaCl, 10 mM Tris-HCl [pH 8.0], 1 mM EDTA), 100 mM sodium carbonate (pH 11.5) or 1% Triton X-100. After incubation at 4°C for 30 min, the samples were subjected to membrane flotation followed by immunoblotting, as described above. Typically, the membrane-bound proteins were associated with fractions 1–4 whereas the soluble proteins were generally present in fractions 5–8, which were followed by the respective protein markers.

Structure predictions and sequence analyses

Multiple sequence alignment and amino acid conservation analyses were performed with the CLUSTALW2 program (Larkin *et al.*, 2007) using the default parameters. The protein secondary structure predictions were generated using DSC (King & Sternberg, 1996), HNN (Guermeur, 1997), MLRC (Guermeur *et al.*, 1999), PHD (Rost, 1996), Jpred 3 (Cole *et al.*, 2008), Porter (Pollastri & McLysaght, 2005), PSIPRED (Jones, 1999) and APSSP2 (Raghava, 2002). The trans-membrane domains were predicted using TopPred II (Claros & von Heijne, 1994). HeliQuest (Gautier *et al.*, 2008) was used for α-helix projections.

ACKNOWLEDGMENTS

We thank Kenneth C. McCullough, Markus Gerber, Sylvie Python, Beatrice Zumkehr, Markus Mader, Daniel Brechbühl, Julie Rappe, Takashi Yamasaki, Shiro Murata and Yuko Okamatsu-Ogura for their excellent contribution and support. We also thank Thomas B. Rasmussen (DTU National

410 Veterinary Institute, Denmark) for providing the plasmid for the transcription of the mono-cistronic
411 replicon rPad2GL, and the late Irene Greiser-Wilke (Community Reference Laboratory for CSF,
412 School of Veterinary Medicine, Hannover, Germany) for mAb HC/TC26.

413 The present work was supported by the Japan Society for the Promotion of Science (JSPS)
414 KAKENHI Grant number 25-1199 to T.T., by the Program for Leading Graduate Schools (F01) from
415 JSPS to T.T., by the Swiss National Science Foundation grant # 310030_141045 to N.R., and by the
416 Swiss Food Safety and Veterinary Office grant # 1.12.20 to N.R. T.T. is supported by JSPS
417 Research Fellowships for young scientists.

REFERENCES

Behrens, S. E., Grassmann, C. W., Thiel, H. J., Meyers, G. & Tautz, N. (1998). Characterization of an autonomous subgenomic pestivirus RNA replicon. *J Virol* **72**, 2364-2372.

Claros, M. G. & von Heijne, G. (1994). TopPred II: an improved software for membrane protein structure predictions. *Computer applications in the biosciences : CABIOS* **10**, 685-686.

Cole, C., Barber, J. D. & Barton, G. J. (2008). The Jpred 3 secondary structure prediction server. *Nucleic acids research* **36**, W197-201.

Dunn, K. W., Kamocka, M. M. & McDonald, J. H. (2011). A practical guide to evaluating colocalisation in biological microscopy. *American journal of physiology Cell physiology* **300**, C723-742.

Egger, D., Wolk, B., Gosert, R., Bianchi, L., Blum, H. E., Moradpour, D. & Bienz, K. (2002). Expression of hepatitis C virus proteins induces distinct membrane alterations including a candidate viral replication complex. *J Virol* **76**, 5974-5984.

Fernandez-Sainz, I., Gladue, D. P., Holinka, L. G., O'Donnell, V., Gudmundsdottir, I., Prarat, M. V., Patch, J. R., Golde, W. T., Lu, Z., Zhu, J., Carrillo, C., Risatti, G. R. & Borca, M. V. (2010). Mutations in classical swine fever virus NS4B affect virulence in swine. *J Virol* **84**, 1536-1549.

Gautier, R., Douguet, D., Antonny, B. & Drin, G. (2008). HELIQUEST: a web server to screen sequences with specific alpha-helical properties. *Bioinformatics* **24**, 2101-2102.

Gladue, D. P., Gavrilov, B. K., Holinka, L. G., Fernandez-Sainz, I. J., Vepkhvadze, N. G., Rogers, K., O'Donnell, V., Risatti, G. R. & Borca, M. V. (2011). Identification of an NTPase motif in classical swine fever virus NS4B protein. *Virology* **411**, 41-49.

Gouttenoire, J., Montserret, R., Paul, D., Castillo, R., Meister, S., Bartenschlager, R., Penin, F. & Moradpour, D. (2014). Aminoterminal Amphipathic alpha-Helix AH1 of Hepatitis C Virus Nonstructural Protein 4B Possesses a Dual Role in RNA Replication and Virus Production. *PLoS pathogens* **10**, e1004501.

Gouttenoire, J., Roingeard, P., Penin, F. & Moradpour, D. (2010). Amphipathic alpha-helix AH2 is a major determinant for the oligomerization of hepatitis C virus nonstructural protein 4B. *J Virol* **84**, 12529-12537.

Greiser-Wilke, I., Moennig, V., Coulibaly, C. O., Dahle, J., Leder, L. & Liess, B. (1990). Identification of conserved epitopes on a hog cholera virus protein. *Arch Virol* **111**, 213-225.

Guermeur, Y. (1997). Combinaison de classifieurs statistiques, application à la prédiction de la structure secondaire des protéines: Université de Paris 6.

Guermeur, Y., Geourjon, C., Gallinari, P. & Deleage, G. (1999). Improved performance in protein secondary structure prediction by inhomogeneous score combination. *Bioinformatics* **15**, 413-421.

Hugle, T., Fehrmann, F., Bieck, E., Kohara, M., Krausslich, H. G., Rice, C. M., Blum, H. E. & Moradpour, D. (2001). The hepatitis C virus nonstructural protein 4B is an integral

endoplasmic reticulum membrane protein. *Virology* **284**, 70-81.

Jones, D. T. (1999). Protein secondary structure prediction based on position-specific scoring matrices. *J Mol Biol* **292**, 195-202.

Kameyama, K., Sakoda, Y., Tamai, K., Igarashi, H., Tajima, M., Mochizuki, T., Namba, Y. & Kida, H. (2006a). Development of an immunochromatographic test kit for rapid detection of bovine viral diarrhea virus antigen. *J Virol Methods* **138**, 140-146.

Kameyama, K., Sakoda, Y., Tamai, K., Nagai, M., Akashi, H. & Kida, H. (2006b). Genetic recombination at different points in the Npro-coding region of bovine viral diarrhea viruses and the potentials to change their antigenicities and pathogenicities. *Virus Res* **116**, 78-84.

King, R. D. & Sternberg, M. J. (1996). Identification and application of the concepts important for accurate and reliable protein secondary structure prediction. *Protein science : a publication of the Protein Society* **5**, 2298-2310.

Knoops, K., Kikkert, M., Worm, S. H., Zevenhoven-Dobbe, J. C., van der Meer, Y., Koster, A. J., Mommaas, A. M. & Snijder, E. J. (2008). SARS-coronavirus replication is supported by a reticulovesicular network of modified endoplasmic reticulum. *PLoS biology* **6**, e226.

Kopek, B. G., Perkins, G., Miller, D. J., Ellisman, M. H. & Ahlquist, P. (2007). Three-dimensional analysis of a viral RNA replication complex reveals a virus-induced mini-organelle. *PLoS biology* **5**, e220.

Lamp, B., Riedel, C., Wentz, E., Tortorici, M. A. & Rumenapf, T. (2013). Autocatalytic cleavage within classical swine fever virus NS3 leads to a functional separation of protease and helicase. *J Virol* **87**, 11872-11883.

Larkin, M. A., Blackshields, G., Brown, N. P., Chenna, R., McGettigan, P. A., McWilliam, H., Valentin, F., Wallace, I. M., Wilm, A., Lopez, R., Thompson, J. D., Gibson, T. J. & Higgins, D. G. (2007). Clustal W and Clustal X version 2.0. *Bioinformatics* **23**, 2947-2948.

Leifer, I., Ruggli, N. & Blome, S. (2013). Approaches to define the viral genetic basis of classical swine fever virus virulence. *Virology* **438**, 51-55.

Lindenbach, B.D., Thiel, H.J., Rice, C.M., (2013). Flaviviridae: The Viruses and Their Replication, p. 712-794. In D.M. Knipe and P.M. Howley (ed), *Fields Virology, 6th ed*., vol. 1. Lippincott-Raven Publishers, Philadelphia, PA.

Mayer, D., Thayer, T. M., Hofmann, M. A. & Tratschin, J. D. (2003). Establishment and characterisation of two cDNA-derived strains of classical swine fever virus, one highly virulent and one avirulent. *Virus Res* **98**, 105-116.

Miller, S., Sparacio, S. & Bartenschlager, R. (2006). Subcellular localisation and membrane topology of the Dengue virus type 2 Non-structural protein 4B. *J Biol Chem* **281**, 8854-8863.

Mittelholzer, C., Moser, C., Tratschin, J. D. & Hofmann, M. A. (1997). Generation of cytopathogenic subgenomic RNA of classical swine fever virus in persistently infected porcine cell lines. *Virus Res* **51**, 125-137.

Mittelholzer, C., Moser, C., Tratschin, J. D. & Hofmann, M. A. (2000). Analysis of classical swine

fever virus replication kinetics allows differentiation of highly virulent from avirulent strains. *Vet Microbiol* **74**, 293-308.

Moser, C., Stettler, P., Tratschin, J. D. & Hofmann, M. A. (1999). Cytopathogenic and noncytopathogenic RNA replicons of classical swine fever virus. *J Virol* **73**, 7787-7794.

Pollastri, G. & McLysaght, A. (2005). Porter: a new, accurate server for protein secondary structure prediction. *Bioinformatics* **21**, 1719-1720.

Qu, L., McMullan, L. K. & Rice, C. M. (2001). Isolation and characterization of noncytopathic pestivirus mutants reveals a role for nonstructural protein NS4B in viral cytopathogenicity. *J Virol* **75**, 10651-10662.

Raghava, G. P. S. (2002). APSSP2 : A combination method for protein secondary structure prediction based on neural network and example based learning. *CASP5* **A**, 132.

Reed, L. & Muench, H. (1938). A simple method of estimating fifty per cent endpoints. *Am J Hyg* **27**, 493-497.

Risager, P. C., Fahnoe, U., Gullberg, M., Rasmussen, T. B. & Belsham, G. J. (2013). Analysis of classical swine fever virus RNA replication determinants using replicons. *J Gen Virol* **94**, 1739-1748.

Romero-Brey, I., Merz, A., Chiramel, A., Lee, J. Y., Chlanda, P., Haselman, U., Santarella-Mellwig, R., Habermann, A., Hoppe, S., Kallis, S., Walther, P., Antony, C., Krijnse-Locker, J. & Bartenschlager, R. (2012). Three-dimensional architecture and biogenesis of membrane structures associated with hepatitis C virus replication. *PLoS pathogens* **8**, e1003056.

Rost, B. (1996). PHD: predicting one-dimensional protein structure by profile-based neural networks. *Methods in enzymology* **266**, 525-539.

Sakoda, Y., Hikawa, M., Tamura, T. & Fukusho, A. (1998). Establishment of a serum-free culture cell line, CPK-NS, which is useful for assays of classical swine fever virus. *J Virol Methods* **75**, 59-68.

Schmeiser, S., Mast, J., Thiel, H. J. & Konig, M. (2014). Morphogenesis of pestiviruses: new insights from ultrastructural studies of strain Giraffe-1. *J Virol* **88**, 2717-2724.

Sharma, R., Ghasparian, A., Robinson, J. A. & McCullough, K. C. (2012). Synthetic virus-like particles target dendritic cell lipid rafts for rapid endocytosis primarily but not exclusively by macropinocytosis. *PLoS One* **7**, e43248.

Spuul, P., Salonen, A., Merits, A., Jokitalo, E., Kaariainen, L. & Ahola, T. (2007). Role of the amphipathic peptide of Semliki forest virus replicase protein nsP1 in membrane association and virus replication. *J Virol* **81**, 872-883.

Tamura, T., Nagashima, N., Ruggli, N., Summerfield, A., Kida, H. & Sakoda, Y. (2014). Npro of classical swine fever virus contributes to pathogenicity in pigs by preventing type I interferon induction at local replication sites. *Vet Res* **45**, 47.

Tamura, T., Sakoda, Y., Yoshino, F., Nomura, T., Yamamoto, N., Sato, Y., Okamatsu, M., Ruggli,

N. & Kida, H. (2012). Selection of classical swine fever virus with enhanced pathogenicity reveals synergistic virulence determinants in E2 and NS4B. *J Virol* **86**, 8602-8613.

Weiskircher, E., Aligo, J., Ning, G. & Konan, K. V. (2009). Bovine viral diarrhea virus NS4B protein is an integral membrane protein associated with Golgi markers and rearranged host membranes. *Virol J* **6**, 185.

Welsch, S., Miller, S., Romero-Brey, I., Merz, A., Bleck, C. K., Walther, P., Fuller, S. D., Antony, C., Krijnse-Locker, J. & Bartenschlager, R. (2009). Composition and three-dimensional architecture of the dengue virus replication and assembly sites. *Cell host & microbe* **5**, 365-375.

Yamasaki, T., Suzuki, A., Shimizu, T., Watarai, M., Hasebe, R. & Horiuchi, M. (2012). Characterization of intracellular localisation of PrP(Sc) in prion-infected cells using a mAb that recognizes the region consisting of aa 119-127 of mouse PrP. *J Gen Virol* **93**, 668-680.

Yu, G. Y., Lee, K. J., Gao, L. & Lai, M. M. (2006). Palmitoylation and polymerization of hepatitis C virus NS4B protein. *J Virol* **80**, 6013-6023.

Zhong, W., Gutshall, L. L. & Del Vecchio, A. M. (1998). Identification and characterization of an RNA-dependent RNA polymerase activity within the nonstructural protein 5B region of bovine viral diarrhea virus. *J Virol* **72**, 9365-9369.

552 ## Figure legends

553 **Figure 1. Schematic representation of the viral genome and of the amino acids of the viral**
554 **proteins relevant for this study**

555 The CSFV genome and the viral proteins N^{pro}, E2 and NS4B of the GPE^- vaccine strain and of
556 the highly virulent Eystrup strain are depicted schematically. The amino acid differences related to
557 virulence reported previously (Tamura *et al.*, 2014; Tamura *et al.*, 2012) and the five additional
558 residues in the N-terminal half of NS4B (2377, 2391, 2398, 2399 and 2414) evaluated in the present
559 study (#) are shown. Numbering starts with the methionine encoded by the AUG start codon.

560

561 **Figure 2. Evaluation of the contribution of NS4B to CSFV pathogenicity**

562 Three groups of six 10-week-old to 13-week-old SPF pigs were inoculated intranasally with $10^{6.0}$
563 $TCID_{50}$ of the parental $vGPE^-$/N136D; T830A; V2475A; A2563V virus, the mutant $vGPE^-$/N136D;
564 T830A; Eystrup NS4B virus and the highly virulent Eystrup strain, respectively. Clinical scores (a),
565 body temperatures (b) and virus titre in the serum (c) were monitored. A body temperature of above
566 40°C was considered fever. At terminal stages of the disease, the animals were euthanized
567 according to defined endpoint criteria (‡) or died unexpectedly (†). The statistical significance of the
568 differences was calculated using the Student's *t*-test. An asterisk indicates significance ($p<0.05$)
569 between the GPE^--derived mutant viruses ($vGPE^-$/N136D; T830A; V2475A; A2563V and
570 $vGPE^-$/N136D; T830A; Eystrup NS4B).

571

572 **Figure 3. Comparison of the effect of NS4B from low and highly virulent CSFV on the**
573 **replication efficiency of GPE^--derived replicons**

574 GPE^--derived bi-cistronic (a) and mono-cistronic (b) luciferase reporter replicons carrying the
575 GPE^- NS4B or its NS4B with the two mutations V2475A and A2563V or the complete NS4B of the
576 highly virulent Eystrup strain were utilized. "#" indicates the locations of the five amino acid
577 differences (2377, 2391, 2398, 2399 and 2414) in the N-terminal domain of these strains.

578 Corresponding bi-cistronic (rGPE$^-$-N^{pro}-Luc-IRES-NS3/GAA) and mono-cistronic (rGPE$^-$-2GL/GAA)
579 replicons encoding an inactive NS5B polymerase were used as controls. After the indicated
580 incubation periods, the firefly luciferase activity from cell lysates (c) and the *Gaussia* luciferase
581 activity from cell culture supernatants (d) was measured as described in METHODS. Results that
582 represented the mean values of the luciferase activity compared with the luciferase activity of the
583 replicons devoid of NS5B polymerase activity at the initial timepoints were obtained from three
584 independent experiments. The error bars represent the standard error. The statistical significance
585 of the differences was calculated using the Student's *t*-test. Significance (p<0.05) is indicated with
586 an asterisk.
587
588 **Figure 4. Comparison of the NS4B amino acid sequences of the low virulent GPE$^-$ and the**
589 **highly virulent Eystrup strains**
590 (a) Based on the secondary structure predictions and their consensus, the α-helices and
591 β-strands are depicted by white columns and arrows, respectively. The trans-membrane domains
592 (TM) are shown with black rectangles. Amino acid numbering started with the beginning of NS4B.
593 The amino acid differences are indicated based on their positions relative to the translation start site
594 of the polyprotein, and they are highlighted in gray. (b) Amphipathic helix wheels in the N-terminal
595 2nd α-helix (α2, amino acid [aa] of NS4B 40–81) of two strains are illustrated, with the amino acid
596 differences indicated by an asterisk. White and black colours indicate hydrophobic and hydrophilic
597 amino acids, respectively. The clustering of hydrophobic, nonpolar residues on one face of the helix
598 suggests an amphipathic configuration. The broken lines separate the two faces of the helix.
599
600 **Figure 5. Role of the predicted N-terminal amphipathic helix domain for protein localisation in**
601 **porcine cells**
602 (a) Schematic representation of the NS4B-GFP chimeric proteins and of the truncated versions
603 expressed from the pCI vector under the control of a cytomegalovirus promoter. The 2nd α-helix

604 domain (aa 40–81) is shown in black. (b) Amino acid sequences and a helical wheel plot of
605 N-terminal domain of NS4B amino acids showing the localisation of the amino acid substitutions for
606 disruption of its amphipathic character. (c) SK-6 cells were transfected with pCI constructs for
607 expression of the indicated NS4B-GFP proteins from the GPE$^-$ strain. GFP fluorescence (green)
608 was analysed by confocal microscopy after 30 h of culture. A plasmid expressing GFP served as
609 control. Nuclei were stained with DAPI (blue). Bars = 10 μm. (d) Membrane flotation analysis of
610 SK-6 cells expressing the N-terminal domain (aa 40–81) of NS4B. SK-6 cells transfected with the
611 pCI vectors, NS4B(40-81)-GFP and its helix mutant, were disrupted mechanically at 36 h after
612 transfection. Equal amounts of postnuclear supernatants were used for membrane flotation and
613 Western blot analysis with an antibody to GFP, GAPDH or calnexin. For the membrane extraction
614 experiments, the postnuclear supernatants were treated with 100 mM Na_2CO_3 (pH 11.5), with 1 M
615 NaCl or with 1% Triton X-100 and subjected to membrane flotation followed by Western blot analysis.
616
617 **Figure 6. Role of the predicted N-terminal amphipathic helix domain for RNA replication**
618 GPE$^-$-derived bi- and mono-cistronic luciferase reporter replicons carrying the mutations for
619 disruption of its amphipathic character were utilized. Respective firefly (a) and *Gaussia* (b)
620 luciferase activities were analysed as described above. Significance (p<0.05) is indicated with an
621 asterisk.
622
623 **Figure 7. Subcellular distribution of the N-terminal domain of NS4B in porcine cells**
624 (a) SK-6 cells were transfected with pCI constructs expressing the NS4B-GFP chimeric proteins.
625 At 36 h after transfection, the cells were processed for live-imaging fluorescence microscopy. The
626 fusion proteins were detected by GFP fluorescence (Green). The ER-Tracker (red) was used as
627 markers for the ER. (b) Co-localisation coefficient with the ER was calculated. Mean and
628 standard deviation of the values acquired from 15 fields of view are depicted.
629

Figure 8. Amino acid alignment of the N-terminal domain (aa 1–81) of CSFV NS4B

The amino acid sequences in the N-terminal domain (aa 1–81) of selected CSFV strains of low, moderate and high virulence were aligned. The hydrophilic amino acids are highlighted in gray. The amino acid differences between the GPE^- and Eystrup strains are marked with an asterisk. A dot indicates the same amino acid as for the GPE^- strain.

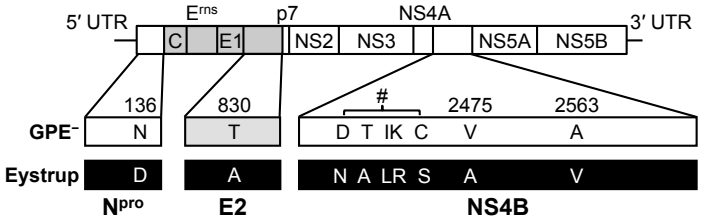

Figure 1. Tamura *et al.*

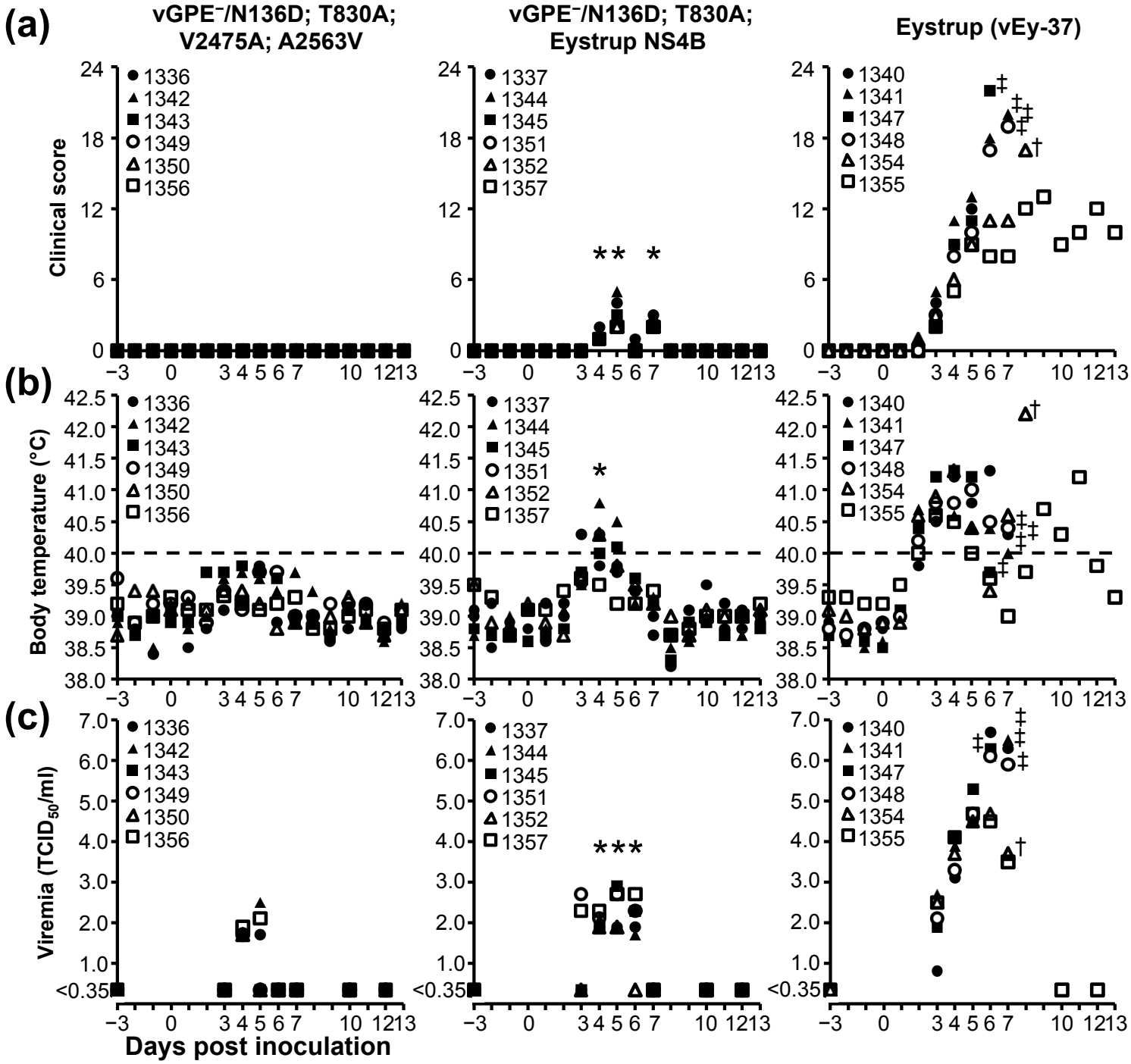

Figure 2. Tamura *et al.*

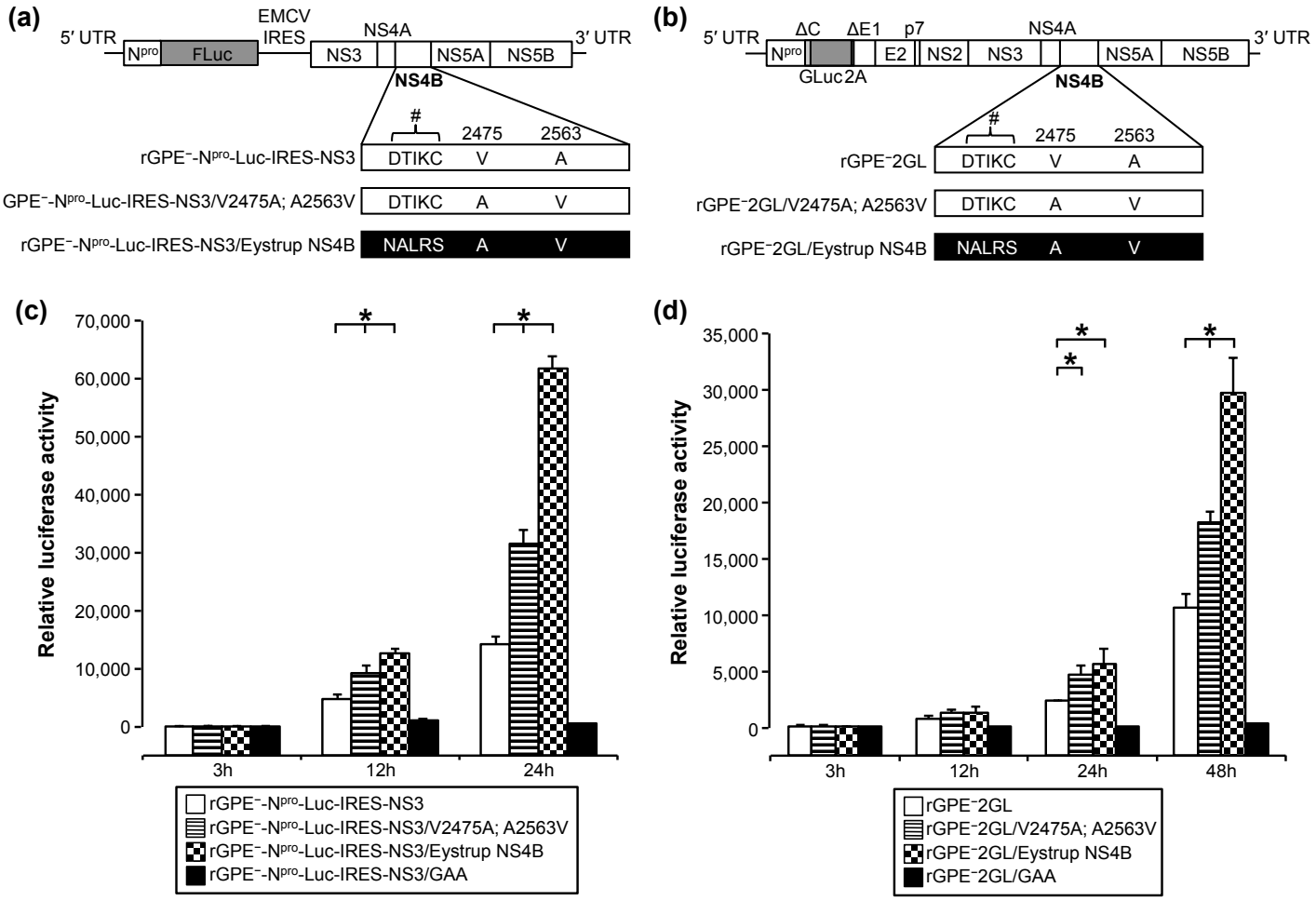

Figure 3. Tamura *et al.*

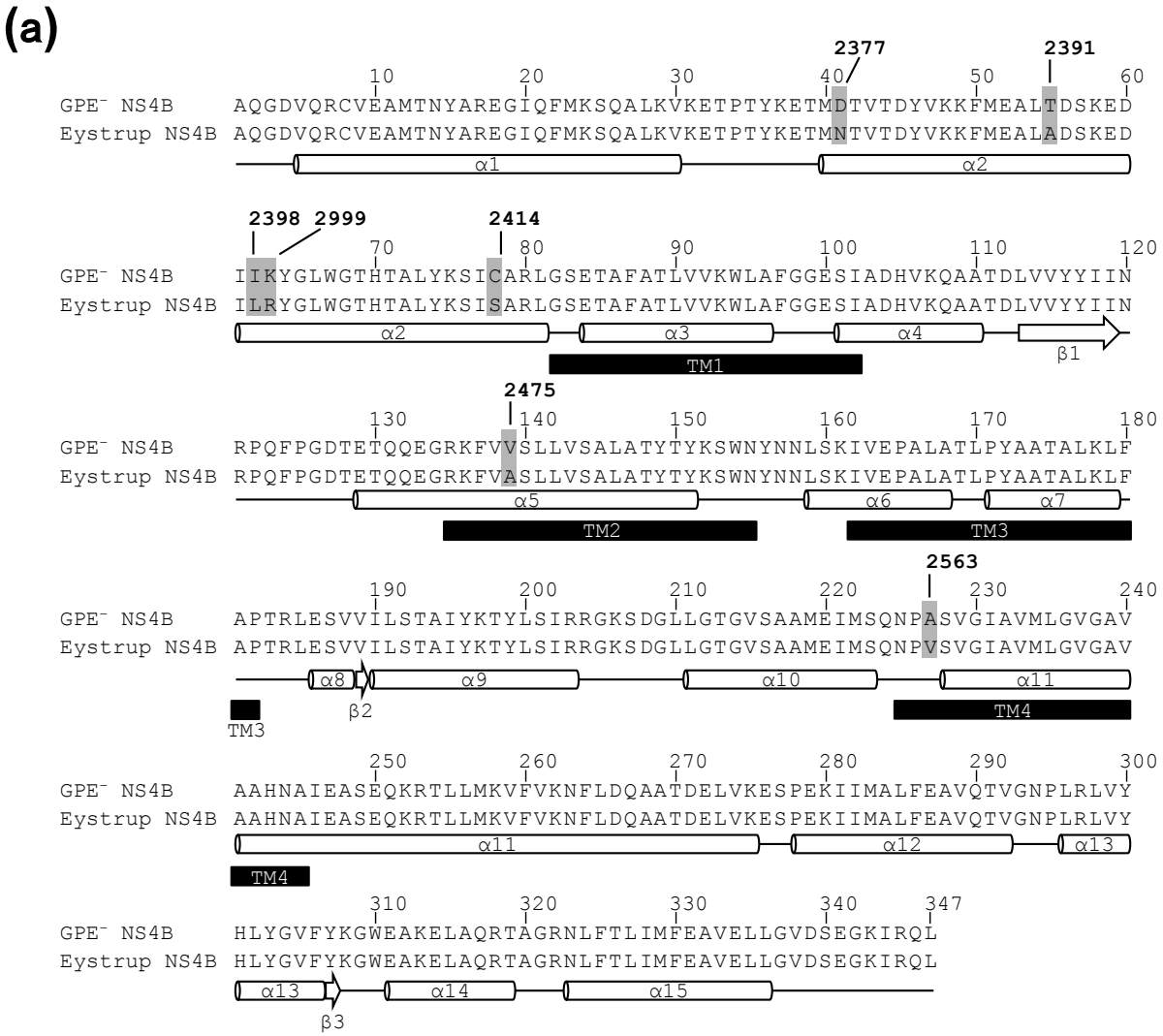

Figure 4. Tamura *et al.*

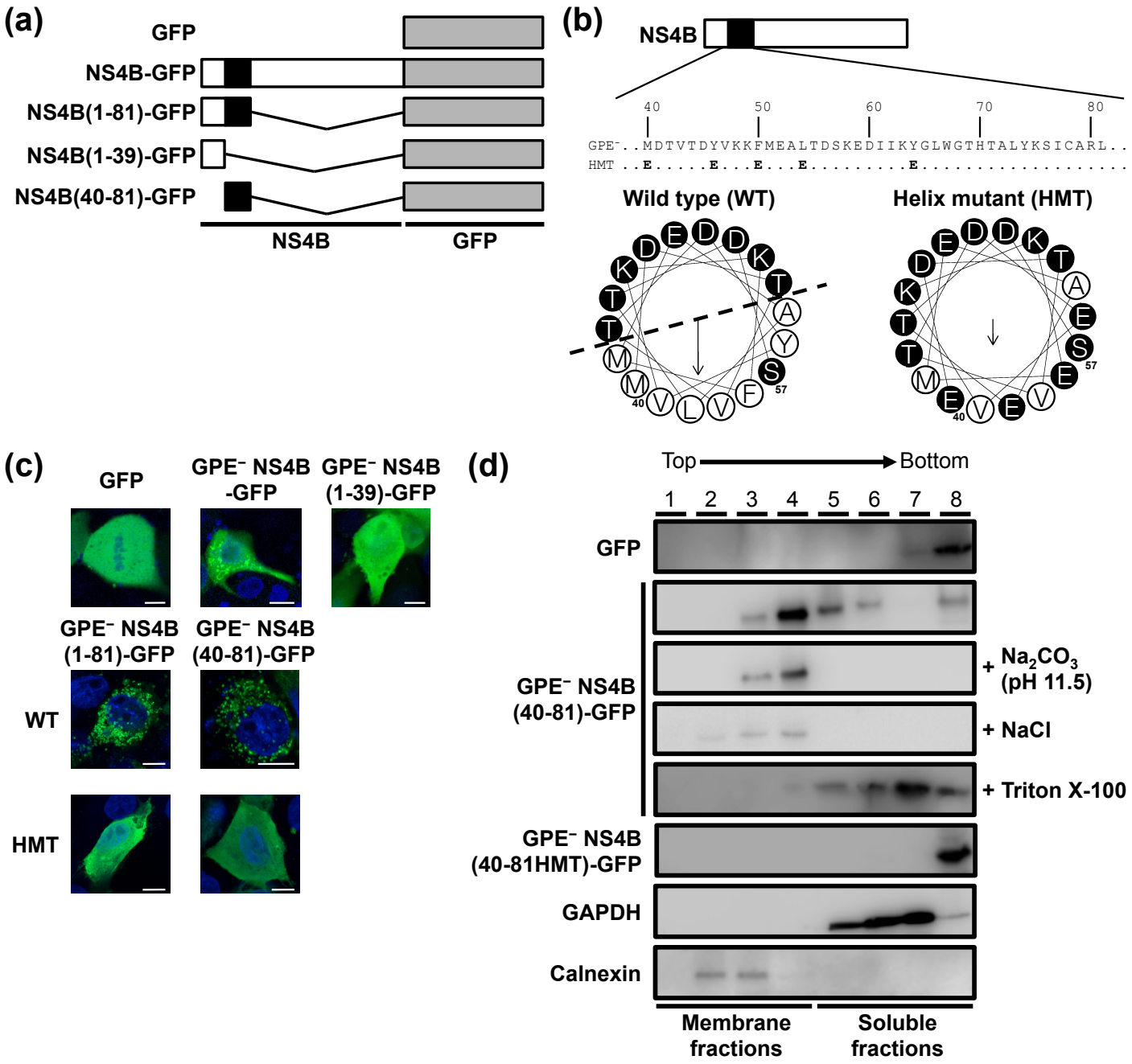

Figure 5. Tamura *et al.*

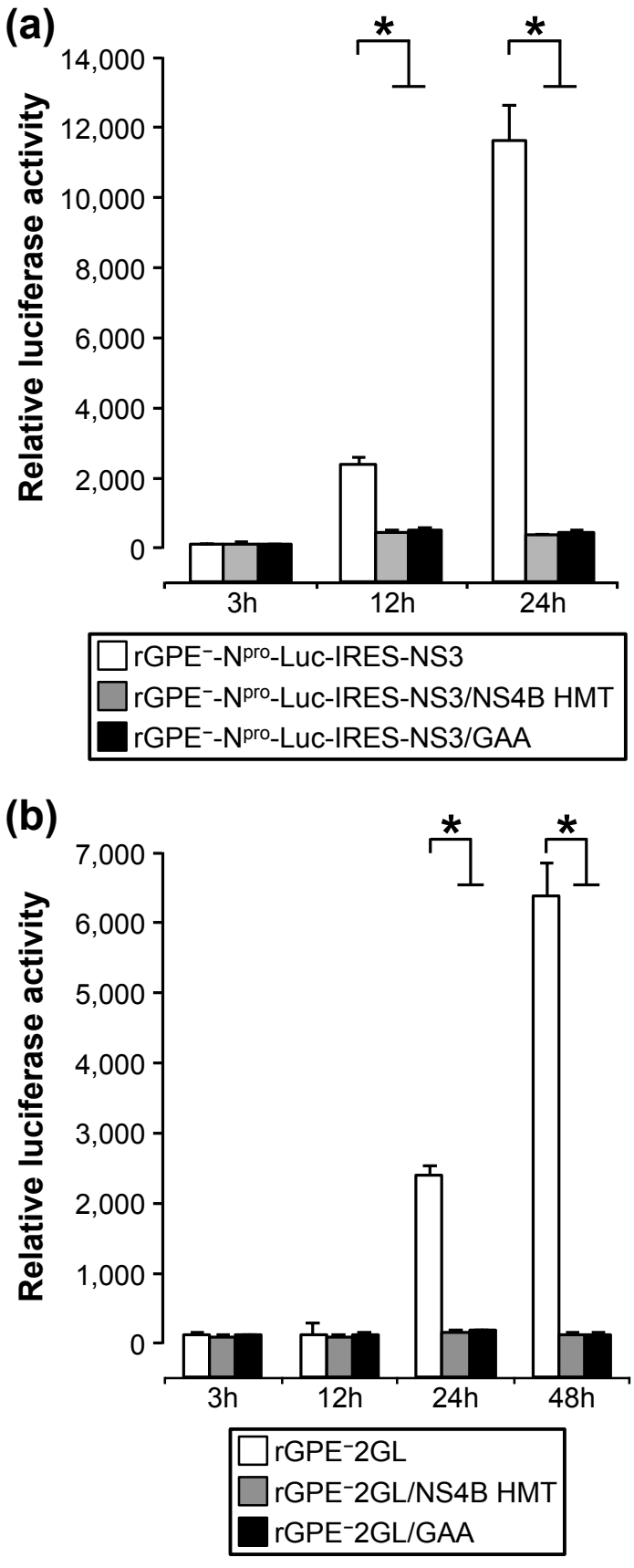

Figure 6. Tamura *et al.*

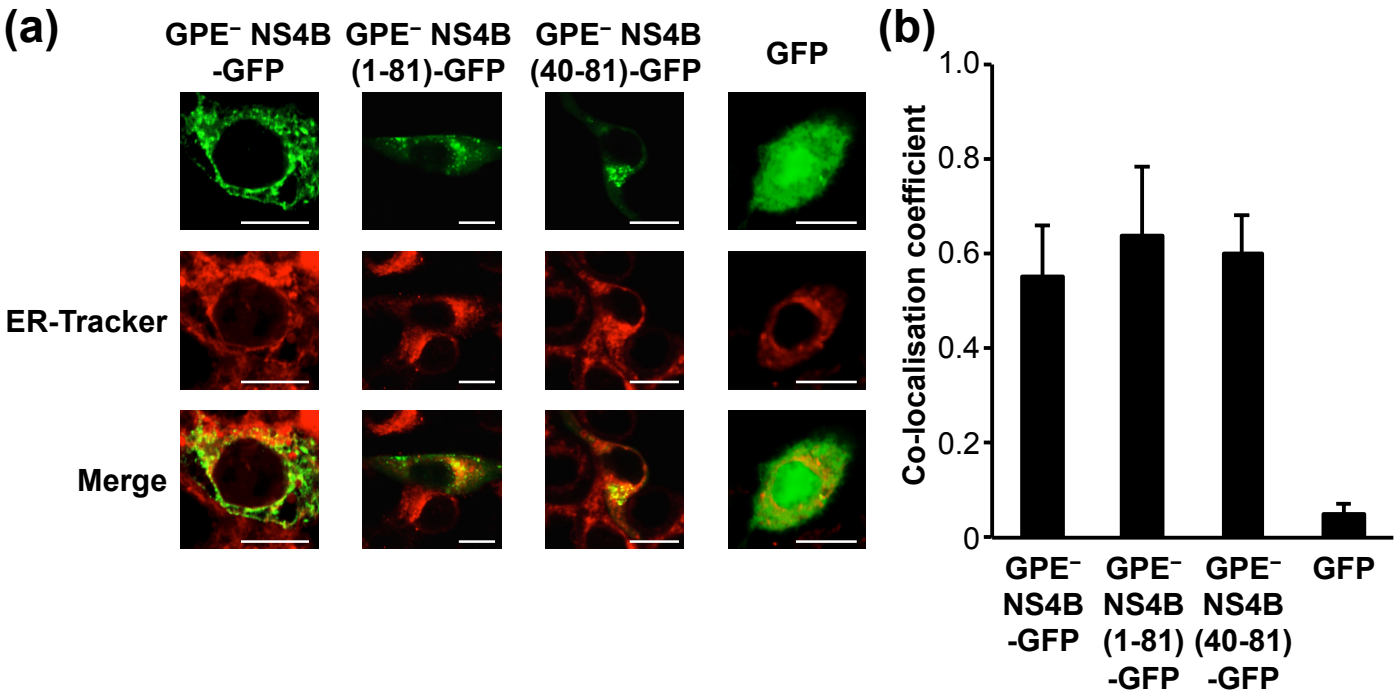

Figure 7. Tamura *et al.*

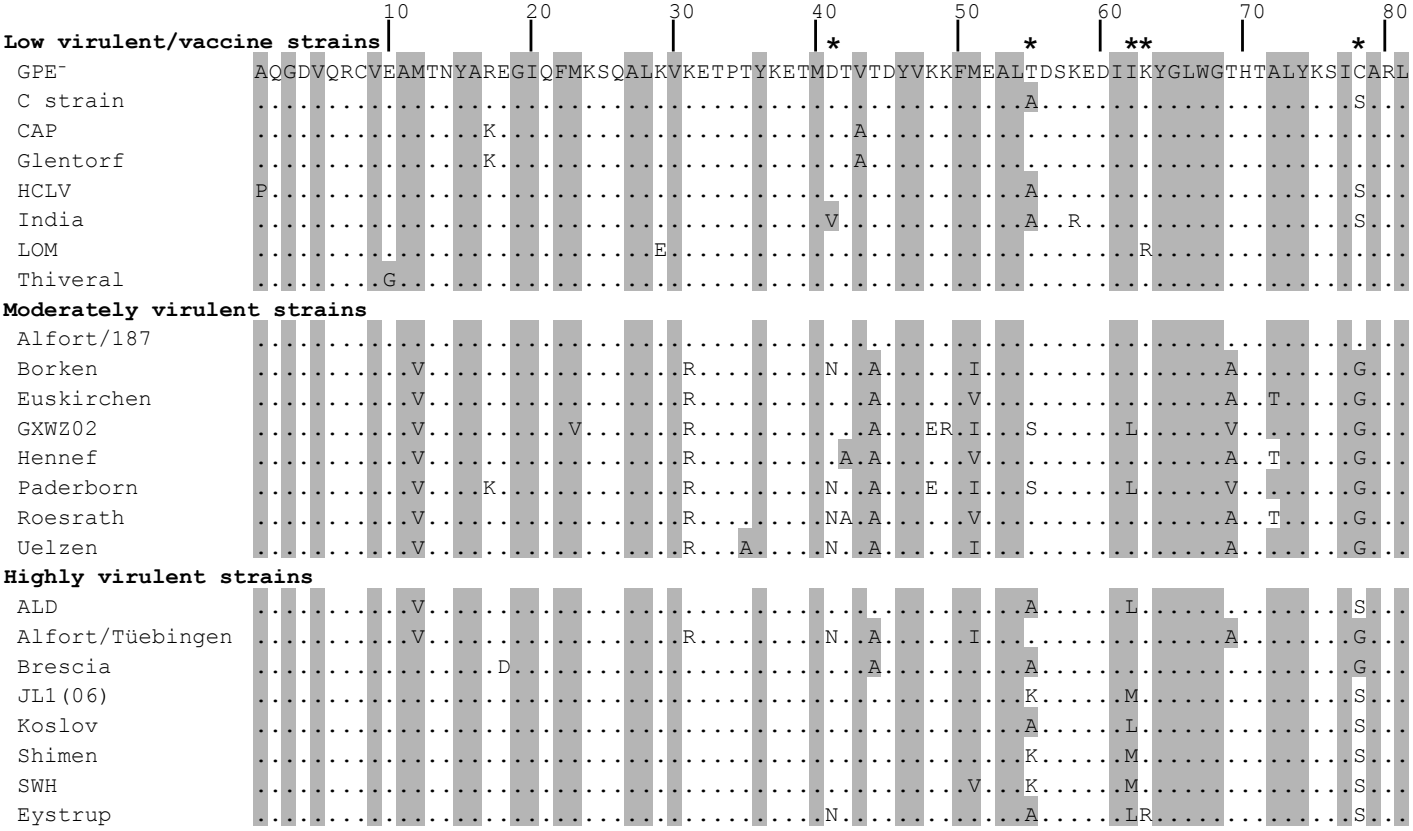

Figure 8. Tamura *et al.*